

Recent Ice-Sheet Growth in the Interior of Greenland

Ola M. Johannessen,^{1,2*} Kirill Khvorostovsky,³ Martin W. Miles,^{4,5} Leonid P. Bobylev³

A continuous data set of Greenland Ice Sheet altimeter height from European Remote Sensing satellites (ERS-1 and ERS-2), 1992 to 2003, has been analyzed. An increase of 6.4 ± 0.2 centimeters per year (cm/year) is found in the vast interior areas above 1500 meters, in contrast to previous reports of high-elevation balance. Below 1500 meters, the elevation-change rate is -2.0 ± 0.9 cm/year, in qualitative agreement with reported thinning in the ice-sheet margins. Averaged over the study area, the increase is 5.4 ± 0.2 cm/year, or ~ 60 cm over 11 years, or ~ 54 cm when corrected for isostatic uplift. Winter elevation changes are shown to be linked to the North Atlantic Oscillation.

The Greenland Ice Sheet is an object of increased attention for at least two reasons related to global climate change (1, 2). First, complete melting of the ice sheet would raise the global sea level up to 7 m. This process, expected to occur on a millennial time scale, should begin when the critical $\sim 3^\circ\text{C}$ threshold for Greenland climate warming is crossed, perhaps before the end of this century (2, 3). Second, increased Greenland Ice Sheet melt and freshwater input into the northern North Atlantic Ocean have been theorized to weaken or even disrupt the global thermohaline circulation on a relatively rapid, multidecadal time scale (4, 5). Here, we address changes in the surface elevation of the interior of the Greenland Ice Sheet, which is pertinent to both of these critical issues through glacier mass balance, i.e., accumulation minus losses.

The response of the Greenland Ice Sheet to climate forcing is not straightforward, because variability in solar radiation, greenhouse gases (GHGs), atmospheric circulation, surface temperature, cloud cover, precipitation, and albedo, as well as glacier-flow dynamics, may affect the magnitude, rate, and direction of changes in glacier mass balance (1–3, 6). Efforts to measure changes in the Greenland Ice Sheet from field observations and aerial and satellite remote sensors have improved our knowledge over the past decade, although there is as yet no consensus assessment of the overall mass balance of the ice sheet (6). There is nonetheless considerable evidence of melting (7–9) and thinning (10, 11) in the coastal marginal areas in recent years, as well as indi-

cations that large Greenland outlet glaciers can surge at subdecadal time scales (12), possibly in response to climate. Less known are changes that may be occurring in the vast elevated interior area of the ice sheet, although a balance has been reported based on some tracks of aerial laser altimetry, unevenly sampled in space and time (10, 13). This underscores the need for long, continuously sampled data sets, such as those derived from satellite altimetry. Whereas decadal and longer satellite-derived data sets have been developed for surface melt (7–9), the surface-elevation data sets analyzed previously have been discontinuous (10, 11, 13) and relatively short (14).

Therefore, we derive and analyze a continuous satellite altimeter height record of Greenland Ice Sheet elevations by combining European Space Agency (ESA) ERS-1 and ERS-2 data to (i) determine the spatial patterns of surface elevation changes over an 11-year period, (ii) determine seasonal and interannual variability of the surface elevation over the same period, and (iii) investigate how observed elevation changes are linked to the North Atlantic Oscillation (NAO) pattern of atmospheric circulation (15), which we hypothesize to have an underappreciated role on the Greenland Ice Sheet surface elevation through its effect on winter precipitation. This is a critical issue, as the NAO index (16) is predicted to become more positive in response to increasing GHGs (17, 18).

The data set analyzed here to identify Greenland Ice Sheet surface-elevation changes is based on 11 consecutive years of ERS-1 and ERS-2 radar altimeter height measurements (19). The methodology used to calculate elevation changes is based on the crossover analysis using the differences in ice-mode altimeter heights at crossing points of the satellite-orbit ground tracks (19). Elevation change rates (dH/dt) were calculated for 0.5° latitude \times 1.0° longitude cells using two methods. In the first method—the dH/dt method (20)—we used all available crossovers. The dH/dt was

determined as a slope of a linear fit to the crossover difference of elevations versus time interval using descending minus ascending orbits. The second method—the time series method (21)—was applied to form seasonally averaged time series of elevation change, using descending minus ascending orbits and ascending minus descending orbits (19). Thus, the first method gives the spatial elevation change averaged for the entire time interval, whereas the second method allows investigation of the temporal variability of spatial averages.

However, to merge ERS-1 and ERS-2 as one data set, it is essential to account for bias between the satellites. To achieve this, we developed and applied the following procedures. We applied the systematic 40.9-cm offset, with ERS-2 being lower than ERS-1, specified by ESA (22) and confirmed by Brenner and colleagues (23), before investigating the remaining bias. Although there was a year (1995 to 1996) when the satellites operated in tandem, the number of ERS-1/ERS-2 crossover points available during this period is considered insufficient to determine the between-satellite bias directly from elevation differences during the overlap (19). Therefore, we estimated the bias using a large number (8 mil-

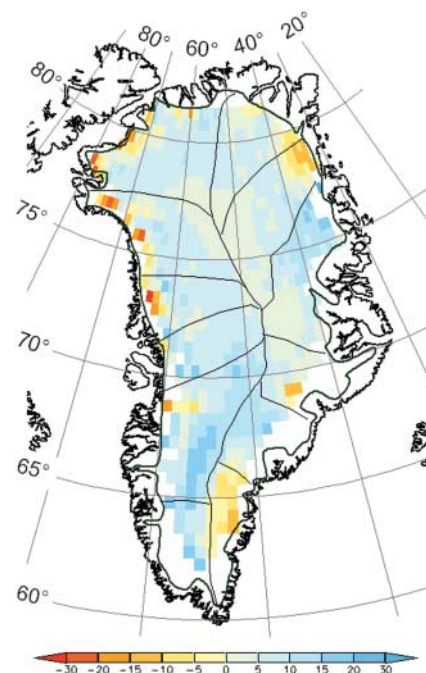


Fig. 1. Greenland, showing the boundaries (thick line) of the ice sheet and major ice divides (thin lines), adapted from (13). The colors indicate ice-sheet elevation change rate (dH/dt) in cm/year, derived from 11 years of ERS-1/ERS-2 satellite altimeter data, 1992 to 2003, excluding some ice-sheet marginal areas (white). The spatially averaged rate is $+5.4 \pm 0.2$ cm/year, or ~ 5 cm/year when corrected for isostatic uplift. The white areas between the color-coded pixels and the thick line delimiting the ice sheet indicate no observations. Latitude in $^\circ\text{N}$, longitude in $^\circ\text{W}$.

¹Mohn-Sverdrup Center for Global Ocean Studies and Operational Oceanography, Nansen Environmental and Remote Sensing Center, Bergen, 5006, Norway. ²Geophysical Institute, University of Bergen, 5007, Norway. ³Nansen International Environmental and Remote Sensing Center, St. Petersburg, 197101, Russia. ⁴Bjerknes Centre for Climate Research, Bergen, 5007, Norway. ⁵Environmental Systems Analysis Research Center, Boulder, CO 80303, USA.

*To whom correspondence should be addressed. E-mail: ola.johannessen@nersc.no

lion) of crossover points between ERS-1 orbits during its whole period of operation from 1992 to 1996 and ERS-2 orbits from a period of equal length, 1995 to 1999, including the 1-year overlap, giving higher reliability (19) (fig. S1). The calculated spatially averaged ERS-1/ERS-2 bias is 21.5 ± 2.0 cm. The bias is spatially variable, and the effect of the bias on determining dH/dt from the crossover data varies from typically ~ 2 cm/year over the interior plateau to about 20 cm/year over ice-sheet margins (19). We applied this bias for each ERS-1 \times ERS-2 crossover point before calculating the dH/dt average for each cell.

The spatial pattern of variability derived from the dH/dt method is mapped as the 11-year elevation-change rate for each cell (Fig. 1), based on 45 million crossover points distributed over three data sets: ERS-1 (ERS-1 \times ERS-1), ERS-2 (ERS-2 \times ERS-2), and ERS-1 and ERS-2 (ERS-1 \times ERS-2). Positive dH/dt values are generally found over most of the high-elevation areas, with largest positive values of up to 10 to 20 cm/year in southwestern ($<69^\circ\text{N}$) and eastern Greenland between 74°N and 77°N . The largest negative values, -25 to -30 cm/year, are found in several parts of western Greenland, where independent aerial altimetry in 1997 and 2002 to 2003 also found the greatest thinning (11). Negative values are also found in southeastern Greenland (63°N to 66°N) and in the northeastern ice stream (78°N to 80°N), with values of -10 to -15 cm/year. The regional differences in elevation change reflect, to varying degrees, the location of ice divides (Fig. 1), notably between southwest and southeast Greenland, $+10$ to $+20$ cm/year and -5 to -15 cm/year, respectively. The most substantial thinning is observed over outlet glacier areas, particularly in western, southeastern, and northeastern Greenland, which implies a dynamic mechanism in addition to changes in precipitation and melting [e.g. (24, 25)].

The surface-elevation change rate averaged over the Greenland Ice Sheet [excluding those marginal cells with unreliable data (19)] is $+5.4 \pm 0.2$ cm/year, or ~ 60 cm for the period 1992 to 2003. We have partitioned the variability into different elevation bands of 500-m intervals, starting at <1500 m and extending to >3000 m (Table 1). Below 1500 m, where summer melting is pronounced, the mean dH/dt is -2.0 ± 0.9 cm/year for the period 1992 to 2003. Above 1500 m, the mean dH/dt is $+6.4 \pm 0.2$ cm/year. These dH/dt values are obtained before correcting for isostatic uplift, which is estimated to be approximately 0.5 cm/year averaged for the entire Greenland Ice Sheet (26). When adjusted for average uplift, the overall ice thickness changes are thus about $+5$ cm/year or 54 cm over 11 years, whereas above 1500 m, these values are about $+6$ cm/year or 65 cm over 11 years. The latter results are in contrast to the

Table 1. Spatially averaged elevation-change rates (dH/dt) and SE partitioned over different elevation bands of the Greenland Ice Sheet, 1992 to 2003, not corrected for isostatic uplift. The uncertainties (\pm) in columns 2 and 3 are SE when averaging results within each band. The values in column 3 are SE of the slope of the linear fit determined for each cell. The areas corresponding to each elevation band are indicated in column 4. These values exclude those cells with unreliable, discarded data (Fig. 1) (19), mostly from the lowest elevation band.

Elevation band (km)	dH/dt (cm/year)	Standard error (cm/year)	Area ($10^3 \times \text{km}^2$)
<1.5	-2.0 ± 0.9	0.4 ± 0.04	155.1
1.5–2	5.6 ± 0.5	0.3 ± 0.03	228.2
2–2.5	7.0 ± 0.4	0.2 ± 0.02	398.9
2.5–3	6.4 ± 0.3	0.2 ± 0.01	458.3
>3	5.5 ± 0.3	0.1 ± 0.01	140.3
All elevation bands	5.4 ± 0.2	0.2 ± 0.01	1380.7

Fig. 2. Interannual variability of spatially averaged Greenland Ice Sheet elevation, shown as anomalies from the 11-year mean, 1992 to 2003. The data are aggregated into areas >1500 m elevation (red) and <1500 m (blue), indicating divergent trends since 2000. The vertical bars indicate SE when averaging the results for each cell.

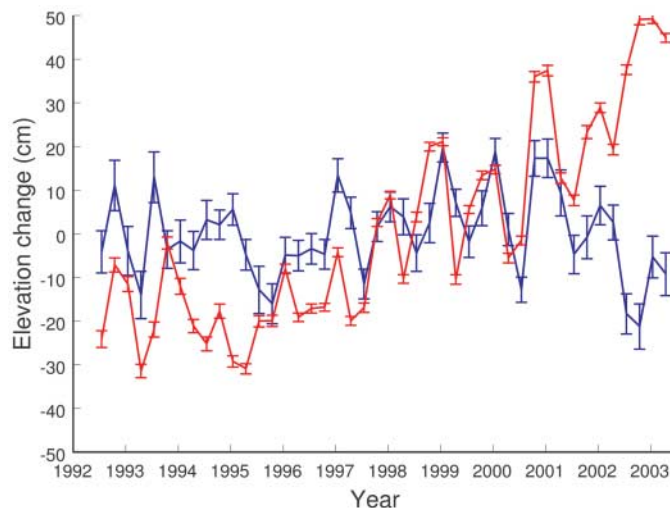
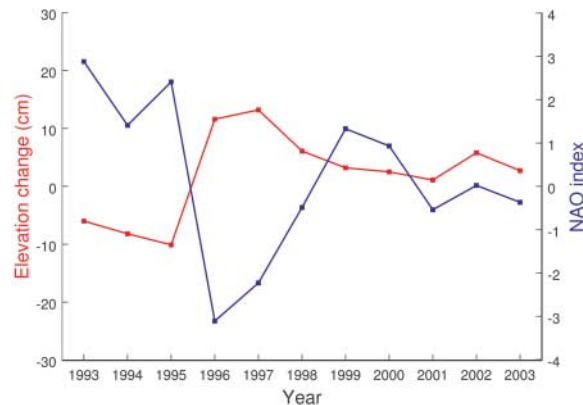


Fig. 3. Spatially averaged changes in winter Greenland Ice Sheet elevation (red) and winter NAO index (blue), lagged 1 month, 1992 to 2003. Winter elevation change during, e.g., 1994/1995 was determined by subtracting autumn 1994 from winter 1994/1995. For elevation, winter is defined as December-January-February with, e.g., winter 1994/1995 specified as 1995. The correlation coefficient between elevation change and the NAO index is -0.88 when lagged 1 month, e.g., November-December-January for the NAO and December-January-February for elevation.



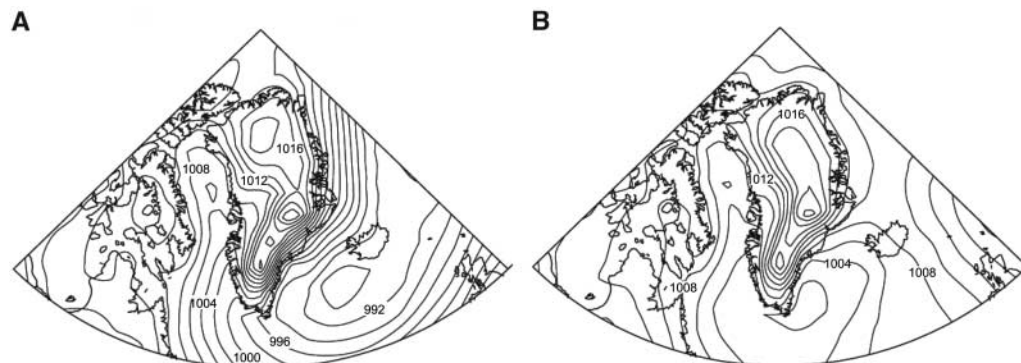
high-elevation balance reported previously (10, 13), based on spatially and temporally discontinuous observations, in contrast to our 11-year data set comprising 45 million crossover points. The positive changes observed here imply increased accumulation, supported by evidence that elevation changes in the interior of Greenland can be attributed primarily to snow accumulation (27).

The time-series analysis (19) of elevation changes spatially averaged over all cells <1500 m and >1500 m indicates seasonal and interannual variability of up to tens of cm (Fig. 2). Below 1500 m, there is no significant

trend until 1999, after which a negative trend of ~ 6 cm/year is evident. Above 1500 m, the positive change is 6.1 ± 0.6 cm/year, confirming the result from the dH/dt method. The overall elevation change derived from the time-series method is $+5.3 \pm 0.5$ cm/year, also confirming the dH/dt result.

Regional temperature and precipitation are both influenced by the NAO (15). Because the NAO in winter strongly affects precipitation, with $r \sim -0.75$ for model-calculated total precipitation for Greenland and $r \sim -0.80$ for southern Greenland (28), we hypothesized that the NAO weather and precipitation pattern

Fig. 4. Composite winter sea-level pressure (mb) in Greenland and surrounding areas (A) 1994/1995 and (B) 1995/1996, which have positive and negative NAO index values, corresponding to negative and positive changes in Greenland Ice Sheet surface elevation, respectively (see Fig. 3). Data are from National Centers for Environmental Prediction (NCEP)/National Center for Atmospheric Research (NCAR) Reanalysis (35).



strongly affects ice-sheet elevation change. However, systematic precipitation measurements are available almost exclusively for the coastal stations and not the interior, such that the NAO index may serve as a proxy for precipitation. Therefore, we examine the direct relation between Greenland Ice Sheet elevation change and the NAO index (16). Elevation changes during winter have been calculated from the time series using the differences between winter (December-January-February) and the preceding autumn (September-October-November). Figure 3 shows ice-sheet elevation changes during winter and the winter NAO index for 1992 to 2003. The correlation between elevation changes and the NAO is maximum when lagged one month, e.g., November-December-January for the NAO and December-January-February for elevation, with $r \sim -0.88$ ($s < 0.05$, $df = 10$), thus explaining about three-quarters ($r^2 \sim 0.77$) of the elevation changes. The correlations for spring, summer, and autumn are, as expected, lower: 0.04, -0.08 , and -0.28 , respectively, implying no significant effect of the NAO during these seasons. The winter correlation (-0.88) is stronger than the above-mentioned correlations for the NAO and modeled Greenland precipitation (28), which implies that the NAO index is a very good proxy for winter precipitation data. Therefore, strongly negative NAO-index conditions lead to increased accumulation and elevation change during wintertime, and vice versa. This is exemplified by the changes observed from 1994/1995 (-10.1 cm) to 1995/1996 ($+11.6$ cm), associated with a record positive-to-negative NAO reversal (2.4σ to -3.1σ) (Fig. 3).

The relation is based not only on the intensity of the NAO but also on the development and position of the Icelandic Low (29), which, for example, shifted southwestward to Cape Farewell between 1994/1995 and 1995/1996 (Fig. 4), giving higher precipitation especially in southern Greenland. However, in other years, a weak negative NAO index may be due simply to a weakly developed Icelandic Low, in which case the elevation change is barely positive, as in 2001 (Fig. 3). The relationship appears weak in the most recent years, since 2001, with the NAO index relatively neutral.

The observed correlation between the NAO and ice-sheet elevation changes suggests that future trends in the NAO could influence the Greenland Ice Sheet surface elevation. The winter NAO index trend has been generally positive since the 1960s, although during our 1992 to 2003 study period, the trend happened to be slightly negative, hence the observed increase in elevation. Model experiments with increasing atmospheric concentrations of GHGs generally indicate an increasing (positive) NAO and a slight northeastward displacement of the Icelandic Low in the future (17, 18)—both implying less winter accumulation over Greenland.

Nonetheless, as mentioned, the NAO can explain about three-quarters of the surface elevation changes, leaving us to speculate on other factors. A modeling study (30) of the Greenland Ice Sheet mass balance under greenhouse global warming has shown that temperature increases up to 2.7°C lead to positive mass-balance changes at high elevations (due to accumulation) and negative at low elevations (due to runoff exceeding accumulation), consistent with our findings, which implies that perhaps a quarter of the growth may be caused by global warming in Greenland (31) in our observation period. Furthermore, the observed elevation change implies that ice-sheet growth in the interior of Greenland may partly offset the freshwater flow of the retreating subpolar glaciers needed to explain the freshening rate of the world ocean, which can be explained almost entirely by Arctic sea-ice melt (32).

In conclusion, we have presented new evidence of (i) decadal increase in surface elevation (~ 5 cm/year) within a study area comprising most of the Greenland Ice Sheet, 1992 to 2003, caused by accumulation over extensive areas in the interior of Greenland; (ii) divergence in elevation changes since the year 2000 for areas above and below 1500 m, with high-elevation increases and low-elevation decreases, the former in contrast to previous research (10, 13); and (iii) negative correlation between winter elevation changes and the NAO index, suggesting an underappreciated role of the winter season and the NAO for elevation changes—a wild card in Greenland Ice Sheet mass-balance scenarios under global warming.

There are, however, caveats to consider. First, we cannot make an integrated assessment of elevation changes—let alone ice volume and its equivalent sea-level change—for the whole Greenland Ice Sheet, including its outlet glaciers, from these observations alone, because the marginal areas are not measured completely using ERS-1/ERS-2 altimetry (see Fig. 1). It is conceivable that pronounced ablation (e.g., 10, 11) in low-elevation marginal areas could offset the elevation increases that we observed in the interior areas. Second, there is large interannual to decadal variability in the high-latitude climate system including the NAO, such that the 11-year-long data set developed here remains too brief to establish long-term trends. Therefore, there is clearly a need for continued monitoring using new satellite altimeters—including advanced ones with improved ice-sheet ranging in steeper coastal areas—and other remote-sensing and field observations, together with numerical modeling to calculate the mass budget through net losses and net input from snow (33).

References and Notes

- Intergovernmental Panel on Climate Change, *Climate Change 2000: Third Assessment Report* (Cambridge Univ. Press, Cambridge, 2001).
- Arctic Climate Impact Assessment, *Impacts of a Warming Arctic* (Cambridge Univ. Press, Cambridge, 2004).
- J. M. Gregory, P. Huybrechts, S. C. B. Raper, *Nature* **428**, 616 (2004).
- S. Rahmstorf, *Clim. Change* **46**, 247 (2000).
- T. Fichefet et al., *Geophys. Res. Lett.* **30**, 10.1029/2003GL017826 (2003).
- E. Rignot, R. H. Thomas, *Science* **297**, 1502 (2002).
- W. Abdulati et al., *J. Geophys. Res.* **106**, 33729 (2001).
- W. Abdalati, K. Steffen, *J. Geophys. Res.* **106**, 33983 (2001).
- K. Steffen, S. V. Nghiem, R. Huff, G. Neumann, *Geophys. Res. Lett.* **31**, L20402 10.1029/2004GL020444 (2004).
- W. Krabill et al., *Science* **289**, 428 (2000).
- W. Krabill et al., *Geophys. Res. Lett.* **31**, L24402, 10.1029/2004GL021533 (2004).
- I. Joughin, W. Abdulati, M. Fahnestock, *Nature* **432**, 608 (2004).
- R. Thomas et al., *J. Geophys. Res.* **106**, 33707 (2001).
- K. Khorostovsky, O. M. Johannessen, L. P. Bobylev, in *Arctic Environmental Variability and Global Change*, L. P. Bobylev, K. Ya. Kondratyev, O. M. Johannessen, Eds. (Springer Praxis, Chichester, UK, 2003), pp. 270–280.
- J. Hurrell, Y. Kushnir, G. Ottersen, M. Visbeck (Eds.), *The North Atlantic Oscillation: Climatic Significance and Environmental Impacts* (American Geophysical Union, Washington, DC, 2003).

16. The NAO index used here is defined as standardized (σ) sea-level pressure (SLP) differences between Iceland and Gibraltar (34).
 17. T. Osborn, *Clim. Dyn.* **22**, 605 (2004).
 18. S. I. Kuzmina et al., *Geophys. Res. Lett.* **32**, L04703, 10.1029/2004GL021064 (2005).
 19. Materials and methods are available as supporting material on Science Online.
 20. H. J. Zwally, A. C. Brenner, J. A. Major, R. A. Bindshadler, J. G. Marsh, *Science* **246**, 1587 (1989).
 21. D. J. Wingham, A. J. Ridout, R. Scharroo, R. Arthern, C. K. Shum, *Science* **282**, 369 (1998).
 22. P. Femenias, ERTNRS-RA-0022, May 1996 http://earth.esa.int/pub/ESA_DOC/QLOPR/er_tn_rs.pdf.
 23. A. C. Brenner, H. J. Zwally, H. G. Cornejo, J. L. Saba, *Proceedings of the ERS-ENVISAT Symposium*, 16–20 October 2000, Gothenburg, Sweden (2000).
 24. R. Layberry, J. Bamber, *J. Geophys. Res.* **106**, 33781 (2001).
 25. C. H. Davis et al., *J. Geophys. Res.* **106**, 33743 (2001).
 26. J. Wahr, T. van Dam, K. Larson, O. Francis, *J. Geophys. Res.* **106**, 33755 (2001).
 27. J. R. McConnell et al., *Nature* **406**, 877 (2000).

28. D. H. Bromwich, Q. S. Chen, Y. F. Li, R. I. Cullather, *J. Geophys. Res.* **104**, 22103 (1999).
 29. J. C. Rogers, D. J. Bathke, E. Moseley-Thompson, S.-H. Wang, *Geophys. Res. Lett.* **31**, L212308, 1029/2004GL021048 (2004).
 30. P. Huybrechts, A. Letreguilly, N. Reeh, *Paleogeogr. Paleoclim. Paleoecol.* **89**, 399 (1991).
 31. P. Chylek, U. Lohmann, *Geophys. Res. Lett.* **32**, L14705, 10.1029/2005GL023552 (2005).
 32. P. Wadhams, W. Munk, *Geophys. Res. Lett.* **31**, L11311, 10.1029/2004GL020039 (2004).
 33. E. Hanna et al., *J. Geophys. Res.* **110**, D13108, 10.1029/2004JD005641 (2005).
 34. P. D. Jones, T. Jónsson, D. Wheeler, *Int. J. Climatol.* **17**, 1433 (1997).
 35. E. Kalnay et al., *Bull. Am. Meteorol. Soc.* **77**, 437 (1996).
 36. Supported by the Research Council of Norway through the "Marine climate and ecosystems in the seasonal ice zone (MACESIZ)" and "Mass balance and freshwater contribution of the Greenland Ice Sheet: A combined modeling and observational approach" projects; the Mohn-Sverdrup Center for Global Ocean Studies and Operational Oceanography; the

International Association for the Promotion of Cooperation with Scientists from the Independent States of the Former Soviet Union (INTAS) through the Fellowship Grant for Young Scientists "Greenland Ice Sheet elevation change and variations derived from satellite altimetry" to K.K. This study was also part of the "Climate and Environmental Change in the Arctic-CECA" project nominated for the European Union Descartes Prize 2005. We also thank ESA and NASA Goddard Space Flight Center for providing processed altimeter data, two anonymous reviewers for helpful comments, and R. J. Telford for language editing.

Supporting Online Material

www.sciencemag.org/cgi/content/full/1115356/DC1
 Materials and Methods

Fig. S1

References

26 May 2005; accepted 11 October 2005

Published online 20 October 2005;

10.1126/science.1115356

Include this information when citing this paper

Ancient DNA from the First European Farmers in 7500-Year-Old Neolithic Sites

Wolfgang Haak,^{1*} Peter Forster,² Barbara Bramanti,¹ Shuichi Matsumura,² Guido Brandt,¹ Marc Tänzler,¹ Richard Villems,³ Colin Renfrew,² Detlef Gronenborn,⁴ Kurt Werner Alt,¹ Joachim Burger¹

The ancestry of modern Europeans is a subject of debate among geneticists, archaeologists, and anthropologists. A crucial question is the extent to which Europeans are descended from the first European farmers in the Neolithic Age 7500 years ago or from Paleolithic hunter-gatherers who were present in Europe since 40,000 years ago. Here we present an analysis of ancient DNA from early European farmers. We successfully extracted and sequenced intact stretches of maternally inherited mitochondrial DNA (mtDNA) from 24 out of 57 Neolithic skeletons from various locations in Germany, Austria, and Hungary. We found that 25% of the Neolithic farmers had one characteristic mtDNA type and that this type formerly was widespread among Neolithic farmers in Central Europe. Europeans today have a 150-times lower frequency (0.2%) of this mtDNA type, revealing that these first Neolithic farmers did not have a strong genetic influence on modern European female lineages. Our finding lends weight to a proposed Paleolithic ancestry for modern Europeans.

Agriculture originated in the Fertile Crescent of the Near East about 12,000 years ago, from where it spread via Anatolia all over Europe (1). It has been widely suggested that the global expansion of farming included not only the dispersal of cultures but also of genes and languages (2). Archaeological cultures such as the Linear pottery culture (*Linearbandkeramik* or LBK) and Alföldi Vonaldiszes Kerámia (AVK) mark the onset of farming in temperate regions of Europe 7500 years ago (3). These early farming cultures originated in Hungary and Slovakia, and the LBK then spread rapidly as far as the Paris Basin and the Ukraine (4, 5). The remarkable speed of the LBK expansion within a period of about 500 years, and the general uniformity of this archaeological unit across

a territory of nearly a million square kilometers (Fig. 1), might indicate that the spread was fueled to a considerable degree by a migration of people (6–8). On the other hand, a number of archaeological studies suggest that local European hunter-gatherers had shifted to farming without a large-scale uptake of genes from the first farmers (9–11). Genetic studies carried out on modern Europeans have led to conflicting results, with estimates of Neolithic input into the present population ranging from 20 to 100% (12–20). A theoretical simulation study by Currat and Excoffier (21) has recently suggested a minor contribution, clearly less than 50%, and possibly much less. Conclusive ancient DNA studies on skeletons of the first European farmers have so far not been published to our knowledge.

To resolve the question regarding the extent of the Neolithic female contribution to the present European population, we collected 57 Neolithic skeletons from 16 sites of the LBK/AVK culture from Germany, Austria, and Hungary. These include well-known archaeological sites such as Flomborn, Schwetzingen, Eilsleben, Asparn-Schletz, and several new excavations; for example, from Halberstadt and Derenburg Meerestieg II. All human remains were dated to the LBK or AVK period (7500 to 7000 years ago) on the basis of associated cultural finds. We extracted DNA from bone and teeth from the morphologically well-preserved individuals, and we amplified nucleotide positions (nps) 15997–16409 [see supporting online material (22)] of the mitochondrial genome with four overlapping primer pairs. In addition, we typed a number of coding-region mtDNA polymorphisms, which are diagnostic for major branches in the mtDNA tree (22).

From a total of 57 LBK/AVK individuals analyzed, 24 individuals (42%) revealed reproducibly successful amplifications of all four primer pairs from at least two independent extractions usually sampled from different parts of the skeleton. Eighteen of the sequences belonged to typical western Eurasian mtDNA branches; there were seven H or V sequences, five T sequences, four K sequences, one J sequence, and one U3 sequence (table S1). These 18 sequences are common and widespread in modern Europeans, Near Easterners, and Cen-

¹Institut für Anthropologie, Johannes Gutenberg Universität Mainz, Saarstrasse 21, D-55099 Mainz, Germany.

²McDonald Institute for Archaeological Research, University of Cambridge, Downing Street, Cambridge CB2 3ER, UK. ³Estonian Biocentre, Tartu University, 23 Riia Str, Tartu, 51010, Estonia. ⁴Römisch-Germanisches Zentralmuseum, Ernst-Ludwig-Platz 2, D-55116 Mainz, Germany.

*To whom correspondence should be addressed at the Molecular Archaeology Group, Institute of Anthropology, Colonel Kleinmann Weg 2, SBII 02, Johannes Gutenberg University, Mainz D-55128, Mainz, Germany. E-mail: haakw@uni-mainz.de